International Journal of Thermophysics, Vol. 11, No. 4, 1990

Fast Transient Thermophysical Measurements at Livermore[1]

G. R. Gathers[2]

The development of the Isobaric Expansion Experiment at Lawrence Livermore National Laboratory is described. Rod samples are self-heated by current from a capacitor bank while current and sample voltage, sample cross section, and temperature are measured continuously as functions of time. The system allows nearly complete thermodynamic characterization of a material along an isobar in a single shot. The pressure of the isobar is determined by containing the sample in argon gas at a predetermined ambient pressure. Correlation of the measured quantities allows elimination of time as a common parameter. Quantities corresponding to a given time are taken to refer to a single equilibrium state. Temperature stagnation and volume and resistivity changes during phase transitions may be seen and allow the heat of transformation and the slope of the phase line in the P, T plane to be determined. Other derived quantities are specific heat c_p, volume-corrected electrical resistivity, and bulk thermal expansion coefficient. A special advantage of the technique is that all quantities are measured on the same sample in a single experiment. The short time duration of the measurements allows access to a temperature range beyond that available to slower methods.

KEY WORDS: electrical resistivity; enthalpy; high-speed methods; high temperature; isobaric expansion; melting; specific heat.

1. INTRODUCTION

New energy technologies typically require unusually high temperatures. This created the need for thermophysical properties data at temperatures beyond the capabilities of conventional steady-state and quasi-steady-state

[1] Paper presented at the First Workshop on Subsecond Thermophysics, June 20–21, 1988, Gaithersburg, Maryland, U.S.A.

[2] Lawrence Livermore National Laboratory, University of California, Livermore, California 94550, U.S.A.

0195-928X/90/0700-0693$06.00/0

techniques. The difficulty is caused by the severe problems created by exposure of the sample and its environment to high temperatures for times of minutes to hours (chemical contamination through reaction with containers, evaporation, loss of electrical insulation and mechanical strength, etc.). As a result, dynamic methods were developed to measure the properties in a very short period of time (less than a second). Cezairliyan [1–3] has reviewed the historical development and details of the dynamic techniques. The microsecond resolution techniques were pioneered by Lebedev and co-workers at the Institute for High Temperatures in Moscow, USSR, as an outgrowth of exploding wire studies [4]. With rapid heating in less than a millisecond, into the liquid state, there is insufficient time for gravity or surface tension to have a significant influence on sample geometry during the measurement period. No container is required in the usual sense, so chemical reaction is essentially eliminated. The early work focused on the heat of fusion and electrical resistivities at the liquidus and solidus for a number of refractory metallic elements and alloys, heated at atmospheric pressure. Temperature was not measured, however, greatly limiting the usefulness of the results.

2. EARLY WORK AT LIVERMORE

A microsecond resolution system was begun at Lawrence Livermore National Laboratory almost concurrently with the work at the Institute for High Temperatures. The initial work was described by Henry et al. [5].

2.1. Apparatus Description

A sample (diameter, 0.1 cm; length, 2.5 cm) was mounted between two clamping jaws in a beryllium high-pressure cell filled with helium gas. Two flash X-ray sources (Blumlein generators) were used to radiograph the sample through the cell at predetermined times to measure the thermal expansion. The sample was self-heated by a current pulse of controlled amplitude and duration from an overdamped capacitor bank (20 kV, 17 kJ) at a rate chosen to avoid nonhomogeneous heating caused by the skin effect and to give nearly isobaric expansion. Two voltage probes spaced 0.5 cm apart contacted the central portion of the sample to avoid the influence of end effects. The energy deposited in the central portion between the probes was calculated by measuring the current through the sample and the potential difference between the probes. These data also allowed the resistance of the sample during most of the heating cycle to be calculated (corrections for self-inductance of the sample are significant at the start of the pulse where the current is low and the rate of increase in

current is at maximum). The heating pulses were in the range of 15- to 40-μs duration. Preliminary measurements were performed on lead at temperatures (estimated) up to 5000 K and pressures to about 200 MPa.

2.2. Problems Encountered

The sample holder was not designed to minimize magnetic deflecting forces on the sample from the heating current. The use of the beryllium pressure cell and flash X-rays also had drawbacks. The X-rays had limited intensity, requiring zinc sulfide intensifying screens in the film packs, degrading resolution. The diverging X-ray beams required magnification calibration, which was crudely accomplished with standard copper rods in the view at the sample holder. Densitometer traces were made to establish the magnification (not very accurate, particularly since the sample had different X-ray cross section). Helium gas was chosen for its low X-ray absorption and was exceedingly difficult to contain in the cell. In addition, the use of the beryllium pressure cell severely restricted the maximum pressure that could be safely used. Because of the snapshot character of the radiographs, only one data point on an isobar could be obtained for a given measurement run. The lack of an optical window prevented the use of a pyrometer.

3. APPARATUS IMPROVEMENTS

3.1. Pressure Cell and Capacitor Bank

Gathers et al. [6–8] eliminated the flash X-ray system and beryllium pressure cell, replacing it with a steel vessel with sapphire windows and backlighting lasers. The optical access allowed both pyrometry and continuous recording of the sample volume using streak camera methods. As a result, data for an entire isobar up to the final state became available from one measurement run. Since helium gas was no longer necessary, argon was substituted, allowing higher confinement pressures. The greater density of the compressed argon also resulted in reduced Taylor instability at the sample surface. Additional changes were a larger capacitor back (45 kJ) and an improved sample holder, which increased the symmetry to reduce deflecting forces on the sample.

3.2. Shadowgraph Systems

Figure 1 gives a schematic of the revised diagnostics. Backlighting for the streak record was provided by a CW argon ion laser. The other line of

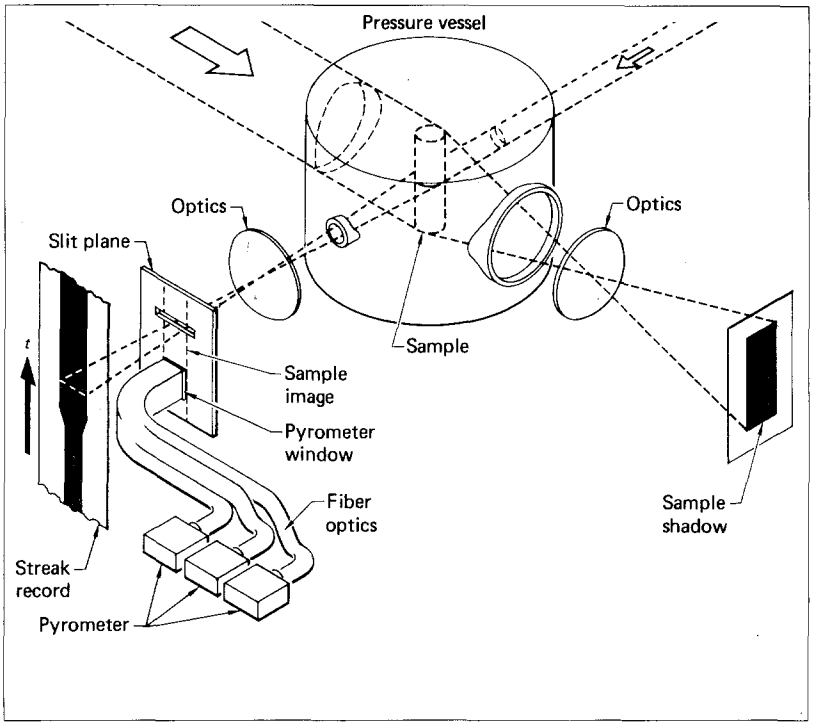

Fig. 1. Schematic of the optical diagnostics of the fast thermophysical measurements system at Livermore. The streak line of sight (LOS) is illuminated continuously with a cw argon ion laser. The other LOS is illuminated with a pulsed ruby laser to take an overall snapshot shadowgraph of the specimen at a late time. The streak record is made with an electronic camera. The snapshot is recorded on film.

sight was used with a Q-switched ruby laser to take an overall snapshot shadowgraph of the sample at a final time in order to detect unstable behavior. Departure from purely radial expansion would make it impossible to determine sample volume from the streak record, and when such behavior was observed, the volume data were discarded. Both the ruby laser shadowgraph and the streak camera system used narrow-band filters to reduce blackbody radiation in competition with the lasers and to reduce interference between the two systems. Both the ruby laser light and the blackbody radiation in the snapshot line of sight were reflected by black glass mirrors on exiting the pressure cell to reduce intensities to photographic levels. This allowed the rest of the optical system to be in air without an air spark at the focal point of lenses in the system. The use of black glass also eliminated second surface reflections at the mirrors.

The use of argon gas in the cell made it necessary to focus the streak system after the cell reached operating pressure. The index of refraction of argon reaches 1.2 at 0.2 GPa. The rapid change in index caused the refraction of light at the gas–sapphire window interface to be a strong function of pressure. Consequently, the magnification of the system was also sensitive to cell pressure. The system was made self-calibrating by starting the streak record before the beginning of the heating current pulse. The snapshot system was designed with a large depth of field to avoid the need for refocusing, and magnification was not required.

3.3. Optical Pyrometer

The pyrometer viewed the sample in the shadow region of the streak system. The viewing area was typically a rectangle about 0.2 cm long and 0.08 cm wide at the sample surface, with the long dimension oriented parallel to the sample axis. The width of the viewing area was determined by an adjustable slit set to exclude light coming from the limb of the sample. This served to prevent possible vignetting effects from sample motion. In addition, possible departures from Lambert's cosine law in that region were avoided. The relatively large viewing area was chosen to increase the sensitivity of the pyrometer enough to use photodiodes rather than photomultipliers as detectors.

Since the light intensity range covered in a measurement run was greater than four orders of magnitude, the output of the detectors was passed through logarithmic amplifiers to reduce the demands on the recording system. Three channels were used with wavelengths centered at 600, 650, and 700 nm with full width at half-maximum of 100 nm. The relatively large passbands served to increase sensitivity. Absolute intensities were not measured. The pyrometer was calibrated using the argon-ion laser as a light source with the sample and narrow-band filters removed. For a given constant output level from the laser, a series of neutral density filters was used to determine the signal levels corresponding to each relative intensity. Curve-fitting methods were used with these data to produce a relative intensity versus voltage transfer function for each channel. The voltage records for a measurement run could then be converted to relative intensity versus time. The need for absolute intensity measurement was eliminated by assigning a temperature to a recognizable feature in the data such as the melting plateau. The output of a single channel can be described by

$$I(T) = G \int \varepsilon(\lambda, T)\, D(\lambda)\, B(\lambda)\, W(\lambda, T)\, d\lambda \tag{1}$$

where $W(\lambda, T)$ is the blackbody spectrum, $D(\lambda)$ is the relative response of the detector, $B(\lambda)$ describes the passband of the filter used, $\varepsilon(\lambda, T)$ is the

emissivity of the sample surface, and G includes such fixed factors as geometric attenuation, scattering losses, etc. The limits of integration are determined by the filter.

If we assume that the emissivity is a weak function of wavelength in the passband, we may take it outside the integral and write the expression as

$$I(T) = G\varepsilon(\bar{\lambda}, T)\, F(T) \tag{2}$$

where

$$F(T) = \int D(\lambda)\, B(\lambda)\, W(\lambda, T)\, d\lambda \tag{3}$$

This function can be calculated in advance for a wide range of temperatures to create a tabular description once the detector and filter functions are specified. As a result, for a given hardware choice, these need not be recalculated during data reduction. Assume that we know the temperature T_c of a characteristic feature such as melting observed in the data, and assume the emissivity to be a linear function of temperature.

$$\varepsilon(\bar{\lambda}, T) = \varepsilon(\bar{\lambda}, T_c)[1 + b(T - T_c)] \tag{4}$$

If $I(T_c)$ is the experimentally observed relative intensity for this feature, we can write

$$G\varepsilon(\bar{\lambda}, T_c) = I(T_c)/F(T_c) \tag{5}$$

and

$$\frac{I(T)}{I(T_c)} = \frac{\varepsilon(\bar{\lambda}, T)}{\varepsilon(\bar{\lambda}, T_c)} \frac{F(T)}{F(T_c)} \tag{6}$$

so that

$$\frac{I(T)}{I(T_c)} = [1 + b(T - T_c)] \frac{F(T)}{F(T_c)} \tag{7}$$

This equation holds for all parts of the pyrometer trace. The left side is the intensity at each point relative to that at the calibrating point. The value of b chosen is that which gives the best overall agreement between the results for two different channels. Emissivity was assumed to be a linear function of temperature and an arbitrary function of wavelength.

All voltage, current, and pyrometer data were recorded using oscilloscopes. Initially, the RF burst produced by the spark gaps of the

capacitor bank provided a cross-timing fiducial for the pyrometer. This proved to be less than satisfactory since the apparent time depended on the intensity setting and writing capability of the oscilloscopes. A fast cross-timing pulse was added to the system to provide a better fiducial.

3.4. Data Obtained from the System

The current data were numerically differentiated for use in making inductance corrections, as were the diameter versus time data obtained from the streak record. During data reduction, an initial inductance was assigned that produced a resistive voltage rising smoothly from zero. The resistive voltage $V(t)$ was then multiplied by the current $I(t)$ to determine the power input versus time to the sample. Since the initial sample density and geometry are known, the sample mass involved could be determined, so that the specific enthalpy is given by

$$h(t) - h(0) = (1/m) \int_0^t I(t)\, V(t)\, dt \tag{8}$$

where m is the mass between the probes, and $h(0)$ is the specific enthalpy at the beginning of the heating cycle.

The temperature versus time record was combined with the enthalpy record to give $h(T)$. A polynomial was fitted to the curve and differentiated to give specific heat $c_p(T)$. Since thermal expansion $v(t)/v_0$ was also measured, one could determine the bulk thermal expansion coefficient as a function of temperature. Sample resistance is given by

$$R(t) = V(t)/I(t) \tag{9}$$

Since the thermal expansion is measured, the true volume-corrected electrical resistivity can also be determined as a function of temperature. When a phase transition (solid–solid, melting) is encountered that produces significant temperature stagnation or kinks in the resistivity, the times for the start and finish of the transition can be determined. The difference between the corresponding enthalpies gives the heat of the transformation. The change in specific volume during the phase change can be used with the Clausius–Clapeyron equation to make an estimate of the pressure derivative of the transition temperature.

Initial attempts at measuring sound velocity in liquid samples in the isobaric expansion experiment were made by Gathers et al. [9] using a displacement interferometer, since it would allow further properties to be determined using the adiabatic compressibility. The Gruneisen parameter can be calculated:

$$\gamma_G = \alpha w^2 / c_p \tag{10}$$

where w is the sound velocity and α is the bulk coefficient of thermal expansion. The specific heat ratio $\gamma = c_p/c_v$ can then be determined from

$$\gamma = 1 + T\alpha\gamma_G \tag{11}$$

The adiabatic compressibility K_s, calculated from the density D and sound velocity w,

$$K_s = 1/Dw^2 \tag{12}$$

can be combined with γ to give isothermal compressibility

$$K_T = \gamma K_s \tag{13}$$

From K_T one can determine the entropy derivative

$$\gamma_v = \left(\frac{\partial S}{\partial v}\right)_T = \frac{\alpha}{K_T} \tag{14}$$

and finally, this can be used to calculate the internal energy derivative

$$\left(\frac{\partial \varepsilon}{\partial v}\right)_T = T\gamma_v - P \tag{15}$$

where P is the ambient pressure of the measurement. The displacement interferometer, however, proved in the end to be too sensitive.

Hixson et al. [10, 11] made improvements to the system and discovered a novel way to measure sound velocity in the liquid sample. A laser-driven stress wave is launched in the sample by focusing the output of a Q-switched ruby laser on one side. The emerging stress wave at the opposite side causes a disturbance in the containment gas that can be detected in the streak shadowgraph record. Some of the ruby laser light is allowed to enter the streak system to serve as a time fiducial. The streak record thus gives the transit time of the stress wave across the diameter of the sample and the average distance traveled. The average sound speed can thus be deduced. The lowest sound speed that can be measured by this technique is determined by the sound speed in the gas. A disturbance in the gas propagates around the perimeter of the sample. The transit time of this wave to the opposite surface must be longer than that for the wave in the sample to cross the diameter.

4. LIMITATIONS OF THE TECHNIQUES

4.1. Instabilities

The practical limit on expansion in isobaric expansion measurements has been determined by the onset of a sudden steep rise in the apparent

resistivity of the liquid metal, accompanied by what appears in shadowgraph records to be sudden rapid acceleration in the radial growth of the sample. The exact nature of this unstable behavior is not well understood.

Martynyuk [12] assumed it to be caused by the final complete loss of stability in a superheated liquid. Figure 2 illustrates his argument. The shaded region is the liquid–vapor coexistence region bounded by the boiling line B–C (binodal), which ends at the critical point C, and the line C–E where condensation from the gas begins. The lines A–C and D–C are the spinodal where

$$\left(\frac{\partial p}{\partial v}\right)_T = 0 \tag{16}$$

At the critical point C the spinodal merges to an inflection point where

$$\left(\frac{\partial^2 p}{\partial v^2}\right)_T = 0 \tag{17}$$

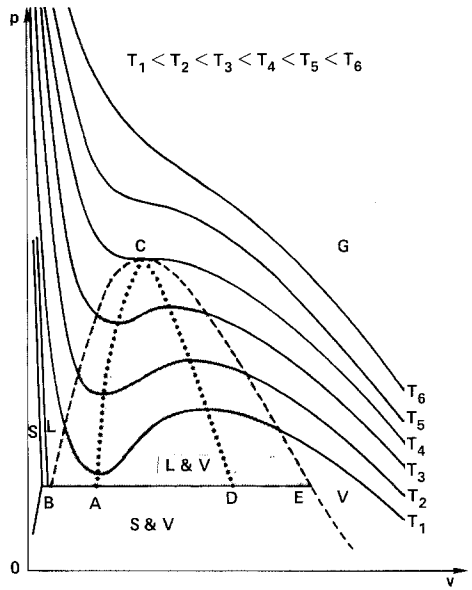

Fig. 2. Isotherms of the classical Van der Waals gas in the P–v plane. The curve BCE bounds the liquid–vapor two-phase region. Curve ACD is the spinodal, bounding mechanically unstable states where compressibility is negative. The point C is the critical point. The region above the critical isotherm T_4 is denoted gas (G). S, L, and V denote solid, liquid, and vapor, respectively.

In the region bounded by the spinodal A–C–D we have

$$\left(\frac{\partial p}{\partial v}\right)_T > 0 \tag{18}$$

which corresponds to negative isothermal compressibility. In this region the liquid is unstable to volume fluctuations. The region between the spinodal and the boiling curve can be composed of either a mixture of liquid and vapor states or superheated liquid states. Martynyuk assumes that heating and expansion have occurred into these superheated states until the spinodal is encountered. The steep rise in resistivity is attributed to density fluctuations. Lebedev et al. [13–16] have also studied the instability and given a rather complex proposed mechanism but not much experimental confirmation. Gathers [17], however, has observed what appears to be the same behavior in copper for expansions well short of the boiling line because of the ambient pressure used.

Hydromagnetic instabilities such as kink and pinch have been observed for low-density, high-conductivity metals. The high current densities required for self-heating result in greater magnetic force and the low density allows instabilities to develop rapidly. Measurements on alkali metals have been quite unsuccessful.

Magnetic diffusion calculations [18, 19] have shown that the increase in resistivity with heating causes the nonuniformity in heating expected from the skin effect to be reduced.

If we assume uniform current density in a cylindrical conductor which has expanded to some radius R at peak current I while immersed in a nonconducting medium which will support pressure, it can be shown that

$$P(R) = P(0) - (I/Rc)^2/2\pi \tag{19}$$

in cgs units, where $P(0)$ is the pressure on the axis, $P(R)$ is the pressure at the conductor surface, and c is the velocity of light in vacuum. It can be seen that for areas where the conductor has a larger radius, pressure on the axis will be reduced. Gathers [17] has observed such difficulties with aluminum. The volume measurements were hampered by an apparent axial movement of liquid metal toward the sample clamping jaws where the pressure is reduced because of the larger conductor radius. We can estimate the pressure gradient in the sample for peak current. In practical units of pressure in Pa, current in A, and R in cm, we have

$$P(0) - P(R) = 1.59375 \times 10^{-4}(I/R)^2 \tag{20}$$

Assume a peak current of 35 kA, an initial sample diameter of 0.1 cm, and twofold expansion at peak current. We have $R = \sqrt{2}\, R_0 = 0.0707$ cm.

$$P(0) - P(R) = 39.1 \text{ MPa } (391 \text{ bar}) \tag{21}$$

For such a system, therefore, we see that the expansion cannot truly be considered isobaric.

4.2. Radiation Losses

For the microsecond systems measurements have been rapid enough to ignore radiation losses. At temperatures above 10000 K, however, the rate of loss will become severe enough to produce substantial temperature gradients in the sample. As a result, the thermophysical measurement will not correspond to a single well-defined state of the material but will represent an average over a mixture of states.

4.3. Electrical Resistivity Bounds

One of the chief limitations of dynamic self-heating methods is that they are limited to conductive materials. If the material is too conductive, the large current densities required to achieve the desired temperatures make the liquid highly susceptible to hydromagnetic instabilities. If the system also uses shadowgraph methods to determine the volume, reducing the sample diameter in order to reduce current requirements also results in a sacrifice of precision in the volume measurements. For a highly resistive material, however, large voltage drops result across the sample. If the sample is in a pressure cell with limited volume, the large voltage developed can make it difficult to prevent arcs between the cell and the sample holding structures. Increasing the volume of the pressure cell to improve electrical insulation requires reducing the pressure capability of the cell for safety reasons, because of limits in the strength of materials. For cells which use a liquid such as water rather than argon gas, the hazards are greatly reduced because far less mechanical energy is stored in the system. The reduced compressibility of the medium, however, results in a measurement that is far from isobaric. To date, this limitation has not been serious because the compressibilities of the metals measured have been too small to make the results sensitive to pressure except as it affects hydromagnetic instabilities.

The electrical resistivity of the material should increase with temperature or the current density in the sample may become nonuniform in a runaway fashion. If a hotter region in the material is more conductive,

current may divert to such a region, producing current filaments in the sample. Evidence of such behavior has been observed in measurements on carbon [7]. Occasional measurements were observed where a localized region of the sample exploded. In materials such as zirconium and titanium [20] resistivity decreases through solid–solid phase transitions, but such regions were traversed in a short enough time that the instability did not develop.

For highly conductive materials the initial resistivity may be increased by alloying methods, reducing the required heating current. Experiments of this kind [17] have been made with Cu–15Ni (15% Ni by wt). Resistivity was increased 10-fold. No significant improvement in sample behavior was observed, however.

The following approximate limits were estimated for the system at Livermore: pressure, 1 GPa; volume, fourfold expansion; temperature, vaporization curve; resistivity, 0.01 $\mu\Omega \cdot$ m. The standard sample diameter was 0.1 cm. For such samples the heating time scale limits were estimated: $t > 10\ \mu$s to avoid inhomogeneous energy deposition due to skin effect; $t < 100\ \mu$s to avoid hydromagnetic instabilities.

4.4. Pyrometer Difficulties

The pyrometer for the Livermore system used logarithmic amplifiers to compress the dynamic range of the recorded data. Experience has shown that this aggravates the calibration difficulties. Most workers have since abandoned the use of log amplifiers for that reason. The pyrometer at Livermore did not make absolute temperature measurements but determined them relative to the known temperature of an observable feature in the data, such as melting. Unfortunately, a calibration error was found in the system due to the use of gelatin neutral density filters in the system for determining the voltage-relative intensity transfer function [21]. The specific heat for tantalum had to be reduced by 14%. All pyrometer measurements of course depend on the model used for the temperature and wavelength dependence of emissivity.

The pyrometer measurements are assumed to be unaffected by glow produced by the thermal excitation of the pressurizing gas. This seems to be a good assumption. The specific heats that have been measured for the hot liquid transition metals have been surprisingly large. Extra light produced by glow would cause the specific heats to appear smaller than they should. In addition, measurements by Gathers [17] on copper produced specific heats in excellent agreement with other results.

4.5. Thermal Expansion in Solid and Liquid

Ivanov et al. [22] questioned whether volumes determined by shadowgraph obtained by Seydel and Kitzel [23] were affected by a thin layer of water vapor propagating ahead of the expanding sample in their cell. The reduced refractive index of the vapor could cause the apparent shadow size to increase. In the system at Livermore the question was raised as the whether a hot layer of argon gas adjacent to the sample would produce the same effect, particularly since coherent radiation was being used. Experiments were performed using simultaneous flash X-ray experiments with the optical shadowgraph. Comparison of the optical and X-ray measurements revealed no significant discrepancy.

Perhaps the most uncertain area arises in the matter of thermal expansion corrections for electrical resistivity. Most authors have made no correction. Those who have did not report the details in the literature. The proper correction depends on the assumptions made about the behavior of the voltage probes and the type of expansion. In the solid, the expansion is almost certainly cubical since the thermal forces involved are much greater than the sample clamps could sustain. In the liquid, the expansion is assumed to be radial, although work by Gathers [17] has shown that it may not always be the case. Since the difference between the two assumptions has been less than the scatter in the data, the matter has been ignored. Corrections in the data from Livermore have always treated the expansion as purely radial. Where it appeared questionable, the results were also reported without corrections. In all cases, the probes are assumed to have a constant amount of material between them, since one could not determine the specific enthalpy otherwise.

5. MATERIALS MEASURED AT LIVERMORE

Table 1 summarizes the measurements made. Shortly after the last entry in the table, the apparatus was dismantled and portions such as the pressure cell were sent to Los Alamos National Laboratory.

The specific heats for transition metals measured in the isobaric expansion experiment at Livermore were surprisingly high. Even after the correction for the calibration error in the pyrometer, these specific heats remain at about 6 to 7R. The results have generally been disregarded by many because the specific heats and heats of fusion are so much greater than for normal metals. Subsequent work by others using a similar apparatus has generally confirmed these high values, however. It is likely that the high values are real. When the Livermore apparatus was used to measure the normal metals Cu and Al, the expected results were obtained.

Table I. Investigations with the Microsecond-Resolution Pulse-Heating System (Isobaric Expansion Experiment) at Lawrence Livermore National Laboratory

Investigator[a]	Ref. No.	Substance	Property[b]	Temperature range (K)[c]
G, S, & Y	6	U	h, v, ρ	(600–5170)
G, S, & Y	7	C	h, v, ρ	(300–8000)
G, S, & Br	8	Ta	h, T	2000–4400
S, G, & M	26	Nb, Mo, Ta, W	Q_m, ρ, v_m, T'_m	Melting temperature
S & G	27	Nb, Mo, Ta, W, U, Pb	α, c, ρ	Liquid range
S, G, & Ho	18	Nb, Mo, Ta, W, U, Pb	Q_m, S_m, c, α	Liquid range
S, G, & Ho	18	Nb, Pb	h, T, v, ρ	Nb: 2300–4110 Pb: 1600–5700
S, G, & M	19	Ta, Mo	h, T, v, ρ, Q_m	Ta: 2200–7400 Mo: 1900–4450
Ho	28	Au–5Cu	h, T, v, ρ	2000–7200
Ho	28	Nb–10Hf–1Ti	h, T, v, ρ	2741–7600
Ho	28	U	h, T, v, ρ	2000–5400
Ho	28	Pb	h, T, v, ρ	1600–5980
G et al.[d]	29	W	h, T, ρ, v, Q_m	2190–5370
G et al.[d]	29	Ta–10W	$h, T, v, \rho, Q_m, V_m, T_m$	2200–7250
G, S, & Ho	30	Pt	$h, T, v, \rho, Q_m, S_m, T'_m$	2100–7300
G, S, Hi, & Y	24	V, Ir	h, T, v, ρ, Q_m	V: 1800–4500 Ir: 2000–7000
G	21	Ta	h, T, c	2000–7250
G	17	Cu, Al	h, T, v, ρ, c	Cu: 2000–4500 Al: 2000–4000
G	20	Ti, Zr	h, v, ρ	Ti: (300–7680) Zr: (300–9350)
G & R	25	Al	T, v, ρ	1000–4000

[a] Author abbreviations are as follows: Br, Brier; G, Gathers; Ho, Hodgson; Hi, Hixson; M, Minichino; R, Ross; S, Shaner; Y, Young.

[b] The property list includes equation-of-state variables when reported. The property symbol designations are as follows: c, heat capacity at constant pressure; α, thermal expansion coefficient; ρ, electrical resistivity; T'_m, pressure derivative of melting temperature; Q_m, heat of fusion; S_m, entropy change during melt; v_m, change in specific volume during melt; h, specific enthalpy; T, temperature; v, specific volume.

[c] Where temperature was not directly measured in the investigation, an estimate was made. Estimates are in parentheses.

[d] Unpublished.

6. CONCLUSIONS

The isobaric expansion experiment at Livermore was a pioneering effort in the use of fast transient methods for thermophysical measurements. A considerable amount of the data produced were the first measurements available in the temperature range considered. The high specific heats seen in the liquid transition metals were an unexpected surprise. Discrepancies between the pyrometer results of various workers remain, but the high specific are seen by all.

ACKNOWLEDGMENT

This work was performed under the auspices of the U.S. Department of Energy by the Lawrence Livermore National Laboratory under Contract W-7405-ENG-48.

REFERENCES

1. A. Cezairliyan, *High Temp. High Press.* **1**:517 (1969).
2. A. Cezairliyan, *Rev. Int. Hautes Temp. Refract.* **7**:215 (1970).
3. A. Cezairliyan, *High Temp. High Press.* **11**:9 (1979).
4. S. V. Lebedev, *High Temp. (USSR)* **6**:150 (1968).
5. K. W. Henry, D. R. Stephens, D. J. Steinberg, and E. B. Royce, *Rev. Sci. Instrum.* **43**:1777 (1972).
6. G. R. Gathers, J. W. Shaner, and D. A. Young, *Phys. Rev. Lett.* **33**:70 (1974).
7. G. R. Gathers, J. W. Shaner, and D. A. Young, *High Temperature Carbon Equation of State*, UCRL-51644 (1974).
8. G. R. Gathers, J. W. Shaner, and R. L. Brier, *Rev. Sci. Instrum.* **47**:471 (1976).
9. G. R. Gathers, J. W. Shaner, C. A. Calder, and W. W. Wilcox, *Proc. 7th Symp. Thermophys. Prop.* (ASME, New York, 1977).
10. R. S. Hixson, M. A. Winkler, and J. W. Shaner, *High Temp. High Press.* **18**:635 (1986).
11. R. S. Hixson, M. A. Winkler, and J. W. Shaner, *Physica* **139/140B**:893 (1986).
12. M. M. Martynyuk, *Sov. Phys.-Tech. Phys.* **19**:793 (1974).
13. S. V. Lebedev, *High Temp. (USSR)* **18**:222 (1980).
14. S. V. Lebedev, *High Temp. (USSR)* **19**:219 (1981).
15. S. V. Lebedev and A. I. Savvatimskii, *High Temp. (USSR)* **8**:494 (1970).
16. S. V. Lebedev and A. I. Savvatimskii, *High Temp. (USSR)* **19**:850 (1982).
17. G. R. Gathers, *Int. J. Thermophys.* **4**:209 (1983).
18. J. W. Shaner, G. R. Gathers, and W. M. Hodgson, *Proc. 7th Symp. Thermophys. Prop.* (ASME, New York, 1977).
19. J. W. Shaner, G. R. Gathers, and C. Minichino, *High Temp. High Press.* **9**:331 (1977).
20. G. R. Gathers, *Int. J. Thermophys.* **4**:271 (1983).
21. G. R. Gathers, *Int. J. Thermophys.* **4**:149 (1983).
22. V. V. Ivanov, S. V. Lebedev, and A. I. Savvatimskii, *J. Phys. F Met. Phys.* **14**:1641 (1984).
23. U. Seydel and W. Kitzel, *J. Phys. F Met. Phys.* **9**:L153 (1979).
24. G. R. Gathers, J. W. Shaner, R. S. Hixson, and D. A. Young, *High Temp. High Press.* **11**:653 (1979).

25. G. R. Gathers and M. Ross, *J. Non-Cryst. Sol.* **61/62**:59 (1984).
26. J. W. Shaner, G. R. Gathers, and C. Minichino, *High Temp. High Press.* **8**:425 (1976).
27. J. W. Shaner and G. R. Gathers, *High Press. Sci. Tech.* **2**:847 (1977).
28. W. M. Hodgson, *Equation of State and Transport Measurements on Expanded Liquid Metals Up to 800 K and 0.4 GPa*, UCRL-52493 (1978).
29. Unpublished.
30. G. R. Gathers, J. W. Shaner, and W. M. Hodgson, *High Temp. High Press.* **11**:529 (1979).